

Formation of anisotropic distributions of mildly relativistic electrons in flaring loops

Victor F. Melnikov, Sergey P. Gorbikov and Nikolai P. Pyatakov

Radiophysical Research Institute,
B.Pecherskaya 25, 603950, Nizhny Novgorod, Russia
email: melnikov@nirfi.sci-nnov.ru

Abstract. In this paper we show that different locations of acceleration/injection sites in flaring loops may produce very different types of pitch-angle distributions of accelerated electrons and, as a consequence, different spatial, spectral and polarization properties of the loop microwave emission. It is shown that these properties can be detected using spatially resolved microwave observations of specific flaring loops and be used to choose the most suitable electron acceleration model.

Keywords. Sun: flares, Sun: radio radiation, acceleration of particles

1. Introduction

Today we know quite a wide variety of acceleration mechanisms in solar flares (see for review [Aschwanden 2002, Vlahos 2007]). Among them are: (1) electric DC-field acceleration (in current sheets or in twisted loops); (2) stochastic acceleration (wave turbulence, micro-flares); (3) shock acceleration (propagating MHD shocks; standing MHD shocks in reconnection outflows); (4) betatron acceleration (in collapsing magnetic traps). Their properties are not the same. They may act and inject accelerated electrons in different places inside a flaring loop, for example, a) *near the loop top* after acceleration in the vertical current sheet (so called 'standard model') or in a strong turbulence region, b) *near a footpoint* of a big loop in a double loop configuration, or c) *along a whole loop* if the loop is twisted or contains numerous micro current sheets. Moreover, different acceleration models may produce electrons with different types of pitch-angle distributions (isotropic, with transverse or parallel anisotropy).

Possibly, all of the mentioned mechanisms may operate in solar flares. Only observations can tell us which mechanism is dominant in a specific flare configuration. Analysis of spatially resolved microwave observations of the Nobeyama Radioheliograph has already allowed to discover very interesting and unexpected phenomena. One of them is the presence of the strong optically thin microwave source in the loop top of some single flaring loops (Kundu *et al.* 2001; Melnikov *et al.* 2002a). Later it was found that such events form quite a numerous class of single flaring loops, about 30-50%, most of others are characterized by the brightness peak(s) close to one or two loop footpoints (Martynova *et al.* 2007; Tzatzakis *et al.* 2006). The phenomenon was explained by the enhanced concentration of mildly relativistic electrons in the upper part of microwave flaring loops (Melnikov *et al.* 2002a). Such looptop electron concentration is possible, if electrons have transverse pitch-angle anisotropy, and particle acceleration/injection takes place near the loop top (Melnikov *et al.* 2006). Another phenomenon is spectral softening of microwave emission near the loop footpoints for disk flares (Yokoyama *et al.* 2002). The discovery was confirmed for other events (Melnikov *et al.* 2002b, Fleishman *et al.* 2003). It was theoretically explained as the spectral softening of gyrosynchrotron (GS) emission

propagating in quasi-parallel direction in the presence of transverse pitch-angle anisotropy of mildly relativistic electrons (Fleishman & Melnikov 2003). Recently, Altyntsev *et al.* (2008) have found ample observational evidences of the existence of parallel to magnetic field pitch-angle anisotropy of energetic electrons in a specific flaring loop. Most interesting evidence of this beam-like anisotropy is the ordinary mode polarization of the emission from optically thin GS microwave source predicted in Fleishman & Melnikov (2003).

The purpose of our paper is to show that the current and future spatially resolved microwave observations are able to provide us with data about the acceleration site and pitch-angle anisotropy of emitting electrons and, therefore, may give us valuable constraints on acceleration models. We focus mostly on the influence of electron distribution dynamics on polarization and spectral properties of GS emission in different parts of a loop.

2. Dynamics of electron distributions

To learn more about the properties of microwave emission and its dynamics in different parts of flaring loops and to study the properties in a more quantitative way than before, we do modelling of the time evolution of the electron spectral, pitch-angle and spatial distributions along a magnetic loop by solving the non-stationary Fokker-Planck equation under different assumptions on the physical conditions in the loop and for different positions of the injection site (loop top, loop legs and feet). We consider the non-stationary Fokker-Planck equation in the form that takes into account Coulomb collisions and magnetic mirroring (Hamilton *et al.* 1990):

$$\begin{aligned} \frac{\partial f}{\partial t} = & -c\beta\mu \frac{\partial f}{\partial s} + c\beta \frac{d \ln B}{ds} \frac{\partial}{\partial \mu} \left[\frac{1 - \mu^2}{2} f \right] \\ & + \frac{c}{\lambda_0} \frac{\partial}{\partial E} \left(\frac{f}{\beta} \right) + \frac{c}{\lambda_0 \beta^3 \gamma^2} \frac{\partial}{\partial \mu} \left[(1 - \mu^2) \frac{\partial f}{\partial \mu} \right] + S, \end{aligned} \quad (2.1)$$

where $f = f(E, \mu, s, t)$ is the electron distribution function of kinetic energy $E = \gamma - 1$ (in units of mc^2), pitch-angle cosine $\mu = \cos \alpha$, distance from the flaring loop center s , and time t , $S = S(E, \mu, s, t)$ is the injection rate, $\beta = v/c$, v and c are the electron velocity and speed of light, $\gamma = 1/\sqrt{1 - \beta^2}$ is the Lorentz factor, $B = B(s)$ is the magnetic field distribution along the loop, $\lambda_0 = 10^{24}/n(s) \ln \Lambda$, $n(s)$ is the plasma density distribution, $\ln \Lambda$ is the Coulomb logarithm.

In this paper we present the results of our numerical experiments only for two cases using the method developed by Gorbikov and Melnikov (2007). In the first case (Model 1) the source of high energy electrons is located in the magnetic trap center $s = 0$, and in the second one (Model 2) near a trap foot $s = 2.4 \times 10^9$ cm. In both models the trap (loop) is symmetrical and its half-length is 3×10^9 cm and magnetic mirror ratio $B_{max}/B_{min} = 2$, $B_{min} = 200$ G. Plasma density is homogeneous along the loop with $n(s) = 5 \times 10^{10} \text{ cm}^{-3}$. The injection function $S(E, \mu, s, t)$ is supposed to be a product of functions dependent only on one variable (energy E , cosine of pitch-angle μ , position s , and time t): $S(E, \mu, s, t) = S_1(E) S_2(\mu) S_3(s) S_4(t)$, where the energy dependence is a power law $S_1(E) = (E/E_{min})^{-\delta}$, $E_{min} = 30$ keV, with the spectral index $\delta = 5$; pitch-angle distribution is isotropic $S_2(\mu) = 1$; time dependence is Gaussian $S_4(t) = \exp[-(t - t_m)^2/t_0^2]$, $t_m = 25$ s, $t_0 = 14$ s; spatial distribution is also Gaussian. For

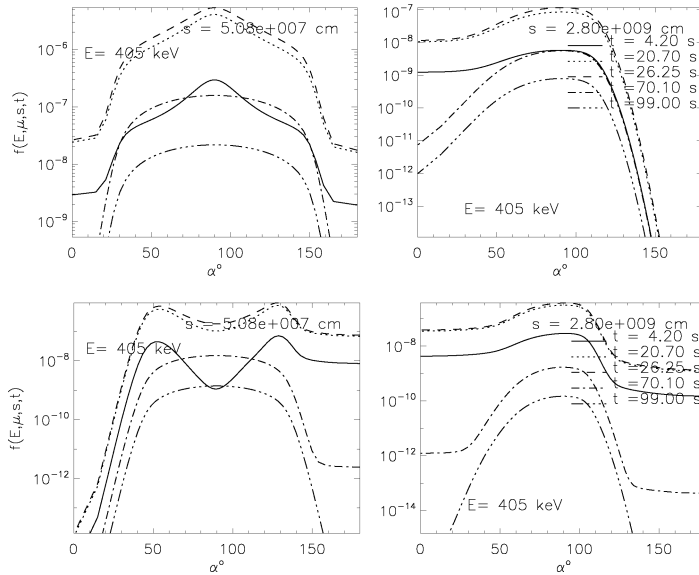


Figure 1. Results of simulations for Model 1 (top panel) and for Model 2 (bottom panel) for electron energy 405 keV and for two positions in the loop: loop top (left panels) and near a footprint (right panels). The distribution functions over pitch-angle α for the rising phase of injection are shown by solid ($t = 4.2$ s), dotted ($t = 20.7$ s) and dashed ($t = 26.25$ s) lines, and for the decay phase by dot-dashed ($t = 70.1$ s) and dot-dot-dot-dashed ($t = 99$ s) lines.

Model 1: $S_3(s) = \exp(-s^2/s_0^2)$, and for Model 2: $S_3(s) = \exp[-(s - s_1)^2/s_0^2]$, where $s_0 = 3 \times 10^8$ cm, $s_1 = 2.4 \times 10^9$ cm.

It is known that spectral and polarization properties of GS emission are very sensitive to peculiarities of the electron pitch-angle distribution in a radio source (Fleishman & Melnikov 2003). So, here, in Fig. 1 we present some results of modelling the pitch-angle distributions of mildly relativistic electrons ($E = 405$ keV) in the center and end of the magnetic trap (loop) for Model 1 and Model 2.

Model 1 (injection at the looptop). In the loop center, the distribution remains anisotropic perpendicular to magnetic field lines during the injection rise, maximum ($t_m = 25$ s) and decay phases. However, the degree of anisotropy decreases with time, especially in the decay phase. Near a loop footprint, the electron pitch-angle distribution is clearly asymmetric, showing a considerable amount of electrons with small pitch-angles. In the decay phase, the distribution becomes more and more symmetric with the peak close to $\alpha = 90^\circ$ (transverse anisotropy increases).

In the case of Model 2 (injection near a footprint), the pitch-angle distribution and its dynamics near the footprint are very similar to the ones in Model 1. At the loop center, however, the shape of the distribution and its dynamics are completely different. First of all, we can see two peaks near pitch-angles 50° and 130° that indicates the presence of oblique fluxes (beams) of electrons. Second, the distribution changes dramatically during the decay time getting more isotropic. Obviously, the pitch-angle scattering due to Coulomb collisions and precipitation into the loss-cone play an important role in the mentioned dynamics.

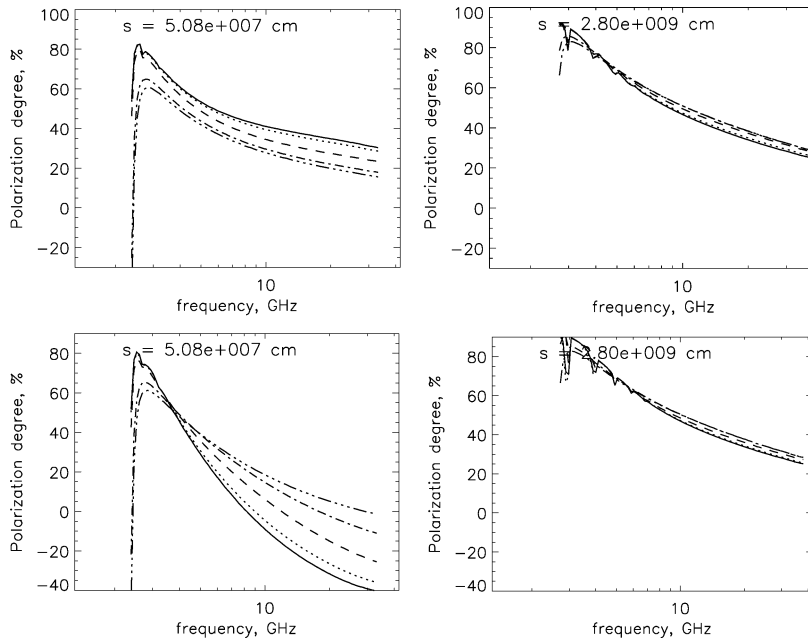


Figure 2. Frequency spectra of polarization degree and its dynamics for Model 1 (top panel) and Model 2 (bottom panel) for two positions in the loop: in the loop top (left plots) and near a footpoint (right plots). The lines meaning is as in Fig. 1.

3. Radio response to the specific electron distributions

In this section we show the influence of electron distribution dynamics on the polarization and spectral properties of microwave GS emission from different parts of a magnetic loop. We do simulations in the frames of assumptions accepted for Model 1 and Model 2 and use the exact formalism described in papers of Ramaty (1969), and Fleishman & Melnikov (2003). The magnetic loop is thin (so that the microwave source is optically thin in the considered frequency range) and located in the plane almost perpendicular to the line of sight ($\theta = 78.5^\circ$).

Results of our simulations are presented in Figs. 2 and 3. Fig. 2 displays frequency spectra of polarization degree and its dynamics for Model 1 (top panel) and Model 2 (bottom panel) for two positions in the loop: in the loop top (left plots) and near a footpoint (right plots). For both models the polarization spectra of emission from the region near a footpoint are very similar. The polarization is positive (X-mode) at all frequencies and its degree is quite high (25 – 30%) even at the highest frequencies. The time evolution is very weak if present at all.

The polarization spectra from the loop top region are markedly different. They show obvious dynamics. They differ from each other. The most striking differences between Model 1 and Model 2 are the following. First, the polarization degree in Model 2 (isotropic injection near a footpoint) is negative (O-mode) at high frequencies, whereas in Model 1 it is positive both at low and high frequencies. Such unusual phenomenon is explained by the fact that in Model 2 we have an oblique flux (beam) of electrons in the central part of the magnetic trap (Fig.1). The oblique beam of energetic electrons is known to produce O-mode polarized emission in the quasi-transverse direction even in optically thin regime (Fleishman & Melnikov 2003). The second strong difference is the difference in the dynamics of the polarization spectra. In Fig. 2 we can see that in Model 1 the

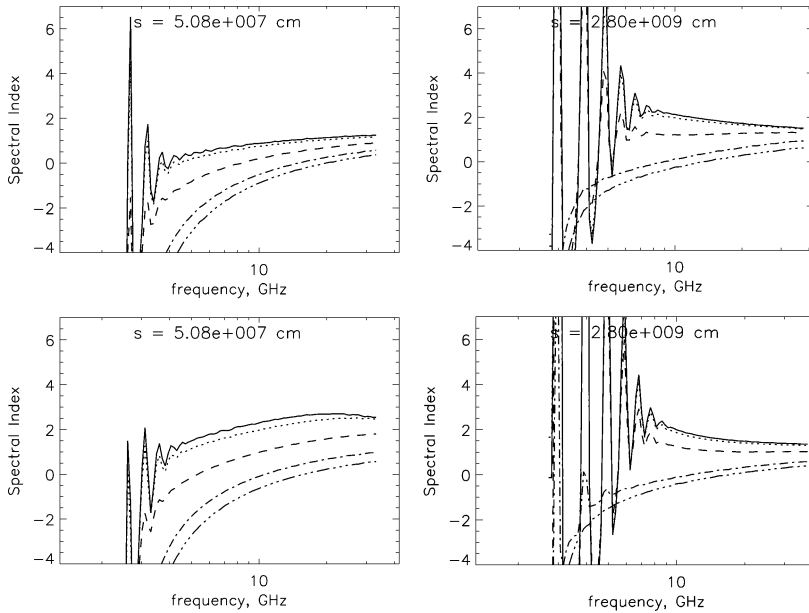


Figure 3. Frequency spectra of the local spectral index $\alpha(f)$. The lines of different styles indicate the moments explained in Fig. 1.

polarization degree decreases with time, by $\approx 10 - 20\%$, whereas in Model 2 it increases considerably, by $\approx 20 - 40\%$, and even may change its sign on the late decay phase of the injection.

Somewhat similar picture of differences between Model 1 and Model 2 is observed for frequency spectra of the local spectral index $\alpha(f)$ and its dynamics (Fig. 3). In Fig. 3 we can see very similar values and dynamics of $\alpha(f)$ near a footpoint (right plots) for both models. At the same time, the values and dynamics of $\alpha(f)$ in the loop top region are noticeably different. For Model 2 the value of $\alpha(f)$ is larger than for Model 1. Moreover, at high frequencies it is even larger than $\alpha(f)$ in the footpoint emission source. The higher values of $\alpha(f)$ in the loop top for Model 2 is definitely associated with the beam-like anisotropy of the energetic electrons in the central part of the magnetic loop (Fig. 1). Such anisotropy is known to produce steeper frequency spectra of GS emission in the quasi-transverse direction (Fleishman & Melnikov 2003).

4. Conclusion

The differences in the behavior of polarization and spectra found for two injection models can serve as a diagnostic tool for distinguishing different types of anisotropic distributions in flaring loops. These findings, together with a set of other recent achievements in the theoretical and observational studies, may be developed into a new method of direct diagnostics of acceleration mechanisms and properties of kinetics of high energy electrons in flaring magnetic loops by means of spatially and spectrally resolved microwave observations. It is clear that building new radio instruments such as FASR, CSRH, and modified SSRT, which are able to observe intensity and polarization of microwave emission in a wide frequency range and with high spatial, spectral and temporal resolution is crucially important for solving the key problems in the physics of solar flare particle acceleration.

The work was partly supported by RFBR grants No.06-02-39029, 06-02-16295, 07-02-01066.

References

- Altyntsev, A. T., Fleishman, G. D., Huang, G. L., & Melnikov, V. F. 2008 *ApJ*, 677, 1367
 Aschwanden, M. J. 2002 *SSRv*, 101, 1
 Fleishman G. D. & Melnikov V. F. 2003 *ApJ*, 587, 823
 Fleishman, G. D., Gary, D. E., & Nita, G. M. 2003 *ApJ*, 593, 571
 Gorbikov, S. P. & Melnikov, V. F. 2007 *Mathematical Modeling*, 19, 112
 Hamilton, R. J., Lu, E. T., & Petrosian, V., 1990 *ApJ*, 354, 726
 Kundu, M. R., Nindos, A., White, S. M., & Grechnev, V. V. 2001 *ApJ*, 557, 880
 Martynova, O. V., Melnikov, V. F., & Reznikova, V. E. 2007 *Proc. of 11th Pulkovo Int. Conf. on Solar Physics, Saint-Peterburg*, 241
 Melnikov, V. F., Shibasaki, K., & Reznikova, V. E. 2002 *ApJ*, 580, L185
 Melnikov, V. F., Reznikova, V. E., Yokoyama, T., & Shibasaki, K. 2002b *ESA*, SP-506, 339
 Melnikov, V. F., Gorbikov, S. P., Reznikova, V. E., & Shibasaki, K. 2006 *Bull. of the RAS Phys.*, 70(10), 1684
 Ramaty R. 1969, *ApJ*, 158, 753
 Tzatzakis, V., Nindos, A., Alissandrakis, C. E., & Shibasaki, K. 2006 *AIP Conf. Proc.*, 848, 248
 Vlahos L. 2007 *Lecture Notes in Physics*, 725, 15
 Yokoyama, T., Nakajima, H., Shibasaki, K., Melnikov, V. F., & Stepanov, A. V. 2002 *ApJ*, 576, L87

Discussion

TERASAWA: Is there a reason why effects of anisotropy driven instabilities, such as whistlers are not included in your analysis? They may not be important in the final anisotropy limit considered.

MELNIKOV: This is an important question. Indeed scattering on whistlers is not included in the Fokker-Plank equation in the form we used. However, we did some calculations and found that for the power-law electron energy distribution the level of generated whistler waves is too weak to scatter resonant relativistic electrons effectively. At least, for the small anisotropy limit considered.

SCHMIEDER: What is the expected spatial resolution of the new generation of radio telescopes in Siberia and with FASR?

MELNIKOV: The angular resolution of FASR is expected to be 1 arcsec at 20 GHz. For the SSRT it will be 10–15 arcsec at the frequency range of 4–9 GHz.

GOPALSWAMY: What is the relation between the microwave loop-top source and the superhot component observed in X-rays?

MELNIKOV: They are coincident. At least for some events we've studied.